Available online at www.sciencedirect.com

ScienceDirect

IFAC PapersOnLine 54-20 (2021) 699–704

Nonparametric continuous-time identification of linear systems: theory, implementation and experimental results

M. Mazzoleni *, **M. Scandella** *, **S. Formentin** **, **F. Previdi** *

* *Department of Management, Information and Production engineering University of Bergamo, via Marconi 5, 24044 Dalmine (BG), Italy (e-mail: mirko.mazzoleni@unibg.it).*
** *Department of Electronics, Information and Bioengineering, Politecnico di Milano, via G. Ponzio 34/5, 20133 Milano, Italy (e-mail: simone.formentin}@polimi.it)*

Abstract: This paper presents an algorithm for continuous-time identification of linear dynamical systems using kernel methods. When the system is asymptotically stable, also the identified model is guaranteed to share such a property. The approach embeds the selection of the model complexity through optimization of the marginal likelihood of the data thanks to its Bayesian interpretation. The output of the algorithm is the continuous-time transfer function of the estimated model. In this work, we show the algorithmic and computational details of the approach, and test it on real experimental data from an Electro Hydro-Static Actuator (EHSA).

Keywords: Software for system identification; Kernel methods.

1. INTRODUCTION

The identification of dynamical systems, due to the intrinsic digital nature of the data, has focused mostly on developing methods for estimating *discrete-time* models. However, discrete-time models present different shortcomings as pointed out in Garnier (2015), since they: (i) depend on the sampling frequency of the data; (ii) are not able to deal with non-uniformly sampled measurements; (iii) cannot easily describe stiff systems; (iv) cannot be easily used for physical insight. *Continuous-time* models can be used to solve such issues since they do not depend on the sampling frequency. Thus, specific approaches were developed for the identification of continuous-time dynamical models, able to deal with uniformly and non-uniformly sampled data, as in Garnier and Wang (2008); Chen et al. (2015).

The above-mentioned identification schemes are mostly *parametric*: they require the prior knowledge of the system structure and order. When this information is not available, complexity measures like the Young Information Criteria (YIC) can be employed, see Young (2011). The YIC works in a similar manner with respect to complexity measures for discrete-time models, such as the Akaike Information Criterion (AIC) or the Bayesian Complexity Criterion (BIC). With this strategy, the model order is selected between a finite set of possible orders (i.e. in a *discrete* way). Instead, non-parametric kernel-based methods tune the model complexity in a *continuous* way. These approaches were introduced in Pillonetto and De Nicolao (2010) for continuous-time LTI systems. The development of the *stable-spline* kernel guarantees the Bounded-Input Bounded-Output (BIBO) stability of the identified model. Kernel methods had a great impact on the community with several contributions also on different regularization, Formentin et al. (2019), and computational aspects, Scandella et al. (2020b).

In order to employ the approach of Pillonetto and De Nicolao (2010), one need to (analytically or computationally) compute the integrals of the input signal $u(t)$ and the kernel function $k(\cdot,\cdot)$. A closed-form formulation of these quantities is possible only for certain simple input signals, see Dinuzzo (2015). For this reason, the following multi-step scheme is usually employed in practice when a continuous-time transfer function is needed: (i) identify a discrete-time regularized high-order Finite Impulse Response (FIR) model; (ii) perform an order reduction of the identified FIR model; (iii) convert the discrete-time reduced model to a continuous-time one.

The proposed algorithm for *direct* (i.e. that avoids multiple steps) nonparametric continuous-time identification of the transfer function of asymptotically stable Single-Input Single-Outout (SISO) Linear Time Invariant (LTI) systems. The method: (i) embeds the automatic selection of the kernel hyperparameters via marginal likelihood optimization; (ii) assures the *asymptotic stability* of the identified model transfer function (provided that the excitation input presents specific properties). In the reported multi-step scheme for continuous-time transfer function computation, the stability property is not guaranteed to be preserved during transformations. So, one benefit of the proposed approach is to have, in one step, a stable model represented as a continuous-time transfer function. This can bee useful, e.g., for control tuning or fault diagnosis.

The proposed scheme has been presented in Mazzoleni et al. (2020), where an *impulse* input is used, and in Scandella et al. (2020a) where also *step* inputs are considered, with a comparison with the `CONTSID toolbox`, developed

Peer review under responsibility of International Federation of Automatic Control.
10.1016/j.ifacol.2021.11.253

by Garnier and Gilson (2018) for continuous-time identification. The contributions of this work are: (i) outline the practical implementation details of our approach; (ii) apply it on a real system using experimental data.

The remainder of this paper is as follows. Section 2 reviews the kernel-based approach for continuous LTI system identification. Section 3 illustrates the estimation method proposed in this paper, based on a step input. Section 4 presents the experimental setup and the identification results. The paper ends with some concluding remarks.

2. IMPULSE RESPONSE IDENTIFICATION

Consider a dataset containing $n \in \mathbb{N} \setminus \{0\}$ noisy measurements, obtained with an experiment on the plant

$$\mathcal{D} = \{(t_i, y_i), 1 \le i \le n\}, \tag{1}$$

distributed according to the probabilistic model

$$y_i = [\breve{g} \star u](t_i) + e_i, \qquad i = 1, \ldots, n \tag{2}$$

where $\breve{g} : \mathbb{R} \to \mathbb{R}$ is the impulse response of a SISO LTI system $\breve{\mathcal{G}}$, $e_i \sim \mathcal{N}(0, \eta^2)$ are independent and identically distributed output-error Gaussian noises, $u : \mathbb{R}_+ \to \mathbb{R}$, y_i, t_i, are, respectively, the *a-priori* known input signal, *measured* output data, and *measured* time instants, with $\star$ denoting the convolution operator [1].

Our purpose is to estimate the (continuous-time) impulse response $\breve{g}$ of $\breve{\mathcal{G}}$ using $\mathcal{D}$ and the knowledge of the analytic expression of $u(t)$. We can then estimate $\breve{g}$ using kernel methods as

$$\hat{g} = \arg \min_{g \in \mathcal{H}_k} \sum_{i=1}^{n} \left(y_i - [g \star u](t_i)\right)^2 + \tau \cdot \|g\|^2_{\mathcal{H}}, \tag{3}$$

where $\mathcal{H}$ is a Reproducing Kernel Hilbert Space (RKHS) with kernel $k(\boldsymbol{\rho}) : \mathbb{R}_+ \times \mathbb{R}_+ \to \mathbb{R}$, $\tau > 0$ controls the regularization strength, $\|\cdot\|_{\mathcal{H}}$ is the induced norm of the space $\mathcal{H}_k$, and $\boldsymbol{\rho} \in \mathbb{R}^{n_\rho \times 1}$ are the hyperparameters of the kernel. According to Dinuzzo and Schölkopf (2012), this estimator can be written as

$$\hat{g}^u(t) = \sum_{i=1}^{n} c_i \hat{g}^u_i(t), \tag{4a}$$

$$\hat{g}^u_i(t) = \int_0^\infty u(t_i - \xi)\, k(t, \xi)\, d\xi. \tag{4b}$$

where the dependency of $\hat{g}^u$ on the $u(t)$ is highlighted. The coefficients vector $\boldsymbol{c} = [c_1, \ldots, c_n]^\top \in \mathbb{R}^{n \times 1}$ can be found by solving the linear system

$$\boldsymbol{O}(\boldsymbol{O} + \tau \boldsymbol{I}_n)\boldsymbol{c} = \boldsymbol{O}\boldsymbol{y}^\top, \tag{5}$$

where $\boldsymbol{y} = [y_1, \ldots, y_n] \in \mathbb{R}^{1 \times n}$ and $\boldsymbol{O} \in \mathbb{R}^{n \times n}$ is a symmetric positive-semidefinite matrix whose (i, j) element is $o^u_{t_i, t_j}$, given by

$$o^u_{t_i,t_j} = \int_0^{+\infty}\int_0^{+\infty} u(t_i - \psi)\, u(t_j - \xi)\, k(\psi, \xi)\, d\xi\, d\psi. \tag{6}$$

[1] We assume that the time instants t_i are in chronological order, i.e. $t_i \ge t_{i-1}$, $i = 2, \ldots, n$ and the excitation signal $u(t)$ is applied to the plant at the time instant $d \in \mathbb{R}$, i.e. $u(t) = 0$, $\forall t < d$, with $t_i > d\ \forall i$.

The estimate $\hat{\boldsymbol{\zeta}}$ of the hyperparameters of $\boldsymbol{\zeta} = \left[\boldsymbol{\rho}^\top, \tau\right]^\top \in \mathbb{R}^{n_\zeta \times 1}$ can be performed by using the Bayesian interpretation of the method, see Pillonetto and De Nicolao (2010):

$$\hat{\boldsymbol{\zeta}} = \arg \min_{\boldsymbol{\zeta} \in \mathbb{R}^{n_\zeta}} \boldsymbol{y}(\boldsymbol{O} + \tau \boldsymbol{I}_n)^{-1} \boldsymbol{y}^\top + \log\det(\boldsymbol{O} + \tau \boldsymbol{I}_n) \tag{7}$$

The choice of the kernel function k is critical for the performance of the estimator (4). In our approach, we employ the *stable-spline kernel*, since it is used in a wide variety of applications. In particular, a *generic order stable-spline kernel* can be represented as follows, see Scandella et al. (2020b):

Proposition 1. (Spline kernels). The spline kernel $s_q : [0, 1] \times [0, 1] \to \mathbb{R}$ and the stable-spline kernel $k_q : \mathbb{R}_+ \times \mathbb{R}_+ \to \mathbb{R}$ of order q can be written, respectively, as:

$$s_q(a, b) = \sum_{h=0}^{q-1} \gamma_{q,h} \begin{cases} a^{2q-h-1} b^h & \text{if } a \le b \\ b^{2q-h-1} a^h & \text{if } a > b \end{cases}, \tag{8}$$

$$k_q(a, b) = \lambda \cdot \sum_{h=0}^{q-1} \gamma_{q,h} \begin{cases} e^{-\beta[(2q-h-1)a + hb]} & \text{if } a \ge b \\ e^{-\beta[(2q-h-1)b + ha]} & \text{if } a < b \end{cases}, \tag{9}$$

where

$$\gamma_{q,h} = \frac{(-1)^{q+h-1}}{h!\,(2q-h-1)!}. \tag{10}$$

Proposition 1 allows to treat the spline order q as an additional hyperparameter, so that $\boldsymbol{\zeta} = [\lambda, \beta, q, \tau]^\top$.

3. TRANSFER FUNCTION IDENTIFICATION

This section reports the main results of the proposed method for continuous-time system identification with kernel methods. For more details, the reader can refer to Scandella et al. (2020a); Mazzoleni et al. (2020).

3.1 *Continuous-time asymptotically stable transfer function estimation: general approach*

The rationale of the proposed approach is depicted Figure 1. The main idea is to compute the Laplace transform $\mathcal{L}$ of (4), to obtain an estimate of the continuous-time transfer function of the system.

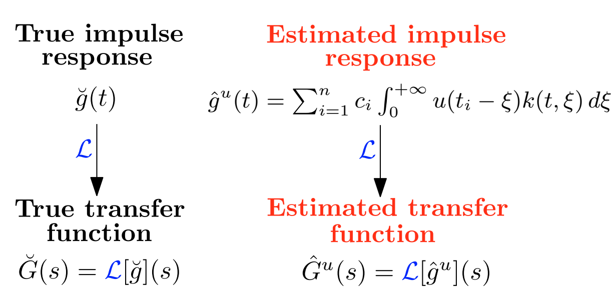

Fig. 1. Rationale of the proposed method.

Proposition 2. (TF expression). Given the continuous-time nonparametric estimator $\hat{g}^u$ in (4) of the impulse response $\breve{g}$ of a continuous-time LTI system $\breve{\mathcal{G}}$, the corresponding continuous-time transfer function estimate is, see Scandella et al. (2020a); Mazzoleni et al. (2020),

$$\hat{G}^u(s) = \sum_{i=1}^{n} c_i \cdot \hat{G}_i^u(s), \tag{11}$$

where

$$\hat{G}_i^u(s) = \int_d^{t_i} u(\tau)\, K(s; t_i - \tau)\, d\tau, \tag{12a}$$

$$K(s; x) = \int_0^{\infty} k(t, x)\, e^{-st}\, dt. \tag{12b}$$

A more informative formulation arises when considering a stable-spline kernel of order q, see Scandella et al. (2020a) and Proposition 1.

Proposition 3. (Stable spline TF expression). Let the kernel be a stable-spline k_q of order q and $u_i(t) = u(t_i - t)$. The identified transfer function can be written as

$$\hat{G}^u(s) = \lambda \cdot \left[\sum_{h=0}^{q-1} Q_{q,h}^u(s) + H_q^u(s) \right], \tag{13}$$

where

$$Q_{q,h}^u(s) = \frac{\gamma_{q,h}}{s + \beta h} \cdot \left(\sum_{i=1}^{n} c_i \cdot A_i^u(\beta(2q - h - 1)) \right) \tag{14a}$$

$$H_q^u(s) = \frac{(-1)^q \beta^{2q-1}}{\prod_{i=0}^{2q-1}(s + \beta i)} \cdot \left(\sum_{i=1}^{n} c_i \cdot A_i^u(s + \beta(2q - 1)) \right) \tag{14b}$$

$$A_i^u(x) = \mathcal{L}[u_i](x). \tag{14c}$$

where $\mathcal{L}$ is the Laplace transform operator.

The following theorem relates the choice of the input signal $u(t)$ with the asymptotic stability of the identified model, see Scandella et al. (2020a).

Theorem 1. (Excitation for stability). If the experiment excitation $u(t)$, used to collect the dataset $\mathcal{D}$, is such that

$$A_i^u\big(s + \beta(2q - 1)\big), \qquad i = 1, \ldots, n \tag{15}$$

are functions whose poles have a negative real part, then the transfer function $\hat{G}^u(s)$ is asymptotically stable.

3.2 Identification using step response data

Consider the case where a step input is applied at the time instant $d \in \mathbb{R}$, i.e.

$$u(t) = \text{step}(t) = \begin{cases} 1 & \text{if } t \geq d \\ 0 & \text{if } t < d \end{cases}, \tag{16}$$

and let

$$\text{step}_i(t) = \text{step}(t_i - t) = \begin{cases} 1 & t \leq t_i - d \\ 0 & t > t_i - d \end{cases} \tag{17}$$

Since $t_i > d$, we have for (14c) that

$$A_i^{\text{step}}(x) = \mathcal{L}[\text{step}_i](x) = \frac{1}{x} - \frac{e^{-x(t_i - d)}}{x} = \frac{1 - e^{-x(t_i - d)}}{x} \tag{18}$$

so that the condition of Proposition 1 is respected.

Applying Theorem 1 and (18), we can to compute the identified transfer function $\hat{G}^{\text{step}}$, see Scandella et al. (2020a)

$$\hat{G}^{\text{step}}(s) = \lambda \cdot \left[\sum_{h=0}^{q-1} Q_{q,h}^{\text{step}}(s) + H_q^{\text{step}}(s) \right] \tag{19a}$$

$$Q_{q,h}^{\text{step}}(s) = \frac{\gamma_{q,h} \sum_{i=1}^{n} c_i \left(1 - e^{-\beta(2q-h-1)(t_i - d)}\right)}{\beta(2q - h - 1)(s + \beta h)} \tag{19b}$$

$$H_{q,h}^{\text{step}}(s) = \widetilde{H}_{q,h}^{\text{step}}(s) \cdot \left(\sum_{i=1}^{n} c_i - T_q^{\text{step}}(s) \right) \tag{19c}$$

$$\widetilde{H}_{q,h}^{\text{step}}(s) = \frac{(-1)^q \beta^{2q-1}}{(s + \beta \cdot (2q - 1)) \prod_{i=0}^{2q-1}(\beta i + s)} \tag{19d}$$

$$T_q^{\text{step}}(s) = \sum_{i=1}^{n} c_i e^{-\beta(2q-1)(t_i - d)} \cdot e^{-s(t_i - d)} \tag{19e}$$

```
%% Compute eq. (18b)
g=@(h)((—1)^(kp.q+h+1)/factorial(h)/factorial(2*kp.q—h—1)); % eq.(10)
%% Define sum(Q(s)), 1st addend of (18a)
Q = tf(0,1); % init transfer function sum(Q(s))
s1 = sum(cc); % 1st addedn of (18b) numerator (sum of coefficients c)
for hh = 0 : 1 : kp.q—1 % from h=1 to h=q—1
    s2 = sum(cc.*exp(—kp.beta.*(2*kp.q—hh—1).*tt)); % 2nd addend of
         the numerator of (18b)
    num = g(hh)*(s1 — s2)/kp.beta/(2*kp.q—hh—1); % numerator of (18b)
    den = [ 1 hh*kp.beta ]; % denominator of (18b)
    Q = Q + tf(num, den); % build 1st term of (18a)
 end
%% define (18e)
T = cc.*exp(—kp.beta.*(2*kp.q — 1).*tt); % term (18e)
T = pade_approximant( tt, T, z ); % see Section 3.3
%% define H(s), 2nd term of (18a)
zH = []; % zeros of (18c)
pH = —kp.beta*(0:(2*kp.q—1)); pH = [ pH pH(end) ]; % poles of (18c)
kH = (—1)^kp.q * kp.beta^(2*kp.q—1); % gain of (18c)
H = zpk(zH, pH, kH) * (s1 — T); %build (18c)
```

The derived kernel (6) in this specific case (i.e. step input signal and stable-spline kernel) reads as

$$o^{\text{step}}(t_i, t_j) = \sum_{h=0}^{q-1} \gamma_{q,h} \begin{cases} w_h(t_i - d, t_j - d) & \text{if } t_i \geq t_j \\ w_h(t_j - d, t_i - d) & \text{if } t_i < t_j, \end{cases}$$

where the term $w_h(a, b)$, when $h = 0$, is equal to

$$w_0(a, b) = 2 \cdot \frac{1 - e^{-\beta b(2q-1)}}{\beta^2 (2q - 1)^2} - b \cdot \frac{e^{-\beta a(2q-1)} + e^{-\beta b(2q-1)}}{\beta(2q - 1)};$$

instead, for $h > 0$, $w_h(a, b)$ is equal to:

$$w_h(a, b) = 2 \cdot \frac{1 - e^{-\beta b(2q-1)}}{\beta^2 (2q - h - 1)(2q - 1)} + \\ - \frac{e^{-\beta a(2q-h-1)}\left(1 - e^{-\beta h b}\right)}{\beta^2 h (2q - h - 1)} + \frac{e^{-\beta b(2q-1)}\left(1 - e^{\beta h b}\right)}{\beta^2 h (2q - h - 1)}.$$

3.3 Padé approximation

The transfer function $H_q^{\text{step}}(s)$ is *not rational* due to (19e). In particular, the numerator is composed by a sum of weighted input-output delays. It is thus useful to obtain a rational approximation using Padé approximant. To do this, restate (19e) as

$$T_q^{\text{step}}(s) = T(s) \equiv \sum_{i=1}^{n} \alpha_i \cdot e^{-s(t_i - d)}. \tag{20}$$

We then have the following result that follows from Baker and Graves-Morris (1996):

Theorem 2. Given the function $T(s)$ in (20), its Padé approximant centered around 0 with $z \in \mathbb{N} \backslash \{0\}$ poles and

z zeros is given by:

$$\widetilde{T}(s) = \frac{\sum_{j=0}^{z} n_j \cdot s^j}{1 + \sum_{j=1}^{z} d_j \cdot s^j}, \tag{21a}$$

$$\boldsymbol{d} = [d_0, \ldots, d_z]^\top = \boldsymbol{A}^{-1}\boldsymbol{b}_2, \tag{21b}$$

$$\boldsymbol{n} = [n_1, \ldots, n_z]^\top = \boldsymbol{b}_1 + \boldsymbol{L}\boldsymbol{d}, \tag{21c}$$

where

$$\boldsymbol{A} = \begin{bmatrix} a_z & a_{z-1} & \cdots & a_1 \\ a_{z+1} & a_z & \cdots & a_2 \\ \vdots & \vdots & \vdots & \vdots \\ a_{2z-1} & a_{2z-2} & \cdots & a_z \end{bmatrix}, \quad \boldsymbol{L} = \begin{bmatrix} 0 & 0 & \cdots & 0 \\ a_0 & 0 & \cdots & 0 \\ a_0 & a_0 & \cdots & 0 \\ \vdots & \vdots & \vdots & \vdots \\ a_{z-1} & a_{z-2} & \cdots & a_0 \end{bmatrix},$$

$$\boldsymbol{b}_1 = [a_0\ a_1\ \cdots\ a_z]^\top, \qquad \boldsymbol{b}_2 = -[a_{z+1}\ a_{z+2}\ \cdots\ a_{2z}]^\top,$$

$$a_j = \frac{1}{j!}\sum_{i=1}^{n} \alpha_i \cdot (d - t_i)^j.$$

The Padé approximation defined in Theorem 2 does not guarantee that $\widetilde{T}(s)$ is stable for every z. For this reason, we started with a value of $z = 25$ and iteratively decrease z until $\widetilde{T}(s)$ is stable.

3.4 Least absolute norm solution

The proposed algorithm requires to solve (5). This linear system can have infinite equivalent solutions, see Scandella et al. (2020b). In this case, we suggest (it is not mandatory) to compute the solution $\boldsymbol{c}_{\mathrm{LN1}}$ with least absolute norm, i.e. such that $\|\boldsymbol{c}\|_1$ is minimum, in order to simplify the computation of the final transfer function estimate. Consider the linear system (5)

$$\boldsymbol{O}\left(\boldsymbol{O} + \tau \boldsymbol{I}_n\right)\boldsymbol{c} = \boldsymbol{O}\boldsymbol{y}^\top, \tag{22a}$$

$$\boldsymbol{B}\boldsymbol{c} = \boldsymbol{b}, \tag{22b}$$

where we defined $\boldsymbol{O}\left(\boldsymbol{O} + \tau \boldsymbol{I}_n\right)\boldsymbol{c} \equiv \boldsymbol{B}$ and $\boldsymbol{O}\boldsymbol{y}^\top \equiv \boldsymbol{b}$. We can employ the Complete Orthogonal Decomposition (COD), see Golub (2013), to decompose $\boldsymbol{B}$ using the quadruple $(\boldsymbol{U}; \boldsymbol{T}; \boldsymbol{V}; r)$ such that:

(1) $r = \mathrm{rank}_\delta \boldsymbol{B}$, where $\mathrm{rank}_\delta \boldsymbol{B}$ denotes the numerical δ-rank of $\boldsymbol{B}$, with δ a threshold;
(2) $\boldsymbol{U}, \boldsymbol{V} \in \mathbb{R}^{n \times r}$ are semi-orthogonal matrices, i.e. $\boldsymbol{U}^\top \boldsymbol{U} = I_r$ and $\boldsymbol{V}^\top \boldsymbol{V} = I_r$;
(3) $\boldsymbol{T} \in \mathbb{R}^{r \times r}$ is a triangular matrix;
(4) $\boldsymbol{B} = \boldsymbol{U}\boldsymbol{T}\boldsymbol{V}^\top$.

Using this decomposition, the linear system (22) can be rewritten as

$$\boldsymbol{T}\boldsymbol{V}^\top \boldsymbol{c} = \boldsymbol{U}^\top \boldsymbol{b}. \tag{23}$$

We used the threshold value δ suggested in (Golub, 2013, Section 5.4.1), see also Scandella et al. (2020c). The $\boldsymbol{c}_{\mathrm{LN1}}$ solution can be computed by solving the optimization problem

$$\boldsymbol{c}_{\mathrm{LN1}} = \arg\min_{\boldsymbol{c} \in \mathbb{R}^{n \times 1}} \|\boldsymbol{c}\|_1 \quad \text{s.t. } \boldsymbol{T}\boldsymbol{V}^\top \boldsymbol{c} = \boldsymbol{U}^\top \boldsymbol{b}, \tag{24}$$

where the constraint is the linear system under analysis written as in (23). We used YALMIP, see Lofberg (2004), equipped with the Gurobi solver for the computation of $\boldsymbol{c}_{\mathrm{LN1}}$, as

```
[U, T, V, ~] = cod(B, eps(norm(B, inf))); % perform COD
x = sdpvar(nt, 1); % define optimization variable
optimize( T*V'*x == U'*b, norm(x,1), hp.yalmip_opt); % optimize
ct = value(x); % get final estimate
```

3.5 Model order reduction

The identified transfer function, especially after the Padé approximation, can have a very high order. It is possible to employ the balance reduction method by Varga (1991) to simplify the model, by using the MatLab command **balred**, along with the command **hsvd** to obtain a list of the singular values $\{\sigma_i\}_{i=1}^{m}$ of the Hankel matrix of a model or system with order m. An effective strategy to choose the reduction order $\bar{m}$ is to first normalize the singular values such that they sum to one, fix a percentage threshold $\lambda_{\mathrm{TH}} \in [0, 1]$, and then retain the least number $\bar{m}$ of singular values such that $\sum_{i=1}^{\bar{m}} \sigma_i \geq \lambda_{\mathrm{TH}}$:

```
TF = ss(TF); % convert estimated transfer function to stae-space
[ s, baldata ] = hsvd(TF); % get Hankel singular values
ninf = sum(isinf(s)); % compute the number of infinite ones
s = s(~isinf(s)); % retain only finite ones
cs = cumsum(flip(sort(s))/sum(s)); % normalize and compute cumsum
o = find(cs > hp.thr_singular_values, 1, 'first'); % find order
TF_red = balred(TF, o + ninf, baldata); % reduce
```

The proposed algorithm is summarized in Algorithm 1.

Algorithm 1 Continuous-time asymptotically stable transfer function estimation

---

Input: The dataset $\mathcal{D}$
Input: A way to compute o^u in (6) given $\boldsymbol{\zeta} = [\lambda, \beta, \tau, q]$ and two time instants
Input: A way to compute $\hat{G}^u$ in (11) given $\boldsymbol{\zeta}$ and $\boldsymbol{c}$
Discard the part of $\mathcal{D}$ corresponding to time instants $t_i \leq d$
Find the optimal hyper-parameters $\hat{\boldsymbol{\zeta}}$ using (7)
Compute the matrix $\boldsymbol{O}$ in (5) using $\hat{\boldsymbol{\zeta}}$ and (6)
Compute a valid solution $\boldsymbol{c}$ of the linear system (5)
Compute $\hat{G}^u$ in (11) given $\hat{\boldsymbol{\zeta}}$ and $\boldsymbol{c}$
[Optional] Perform a Padé approximation of $\hat{G}^u$ with (21)
[Optional] Reduce the model with balanced reduction
Output: The continuous-time transfer function $\hat{G}^u$

Remark 1. The computational complexity of the proposed method does not differ significantly with respect to traditional kernel methods, because the most time-consuming tasks are the computation of (5) and optimization of (7).

4. EXPERIMENTAL SETUP AND RESULTS

We tested the approach on a Electro HydroStatic Actuator (EHSA), based on a closed-circuit hydraulic transmission and a BrushLess DC (BLDC) electrical motor. The BLDC is directly connected to a bidirectional fixed displacement gear pump, that modulates the oil flow and pressure inside the two chambers of a hydraulic cylinder, see Figure 2.

The rotation of the motor-pump assembly determines (i) the oil flow in the cylinder chambers and (ii) an increase of the differential pressure in the hydraulic cylinder. The pressure applied to the piston surface generates a force that acts on the actuator rod. A safety circuit is present to alleviate the risks of pump cavitation and damage in particular operating conditions. The safety circuit is made by over-load valves and anti-cavitation valves that give access to a small oil tank to restore the hydraulic circuit pressure to its nominal range. In this configuration, the

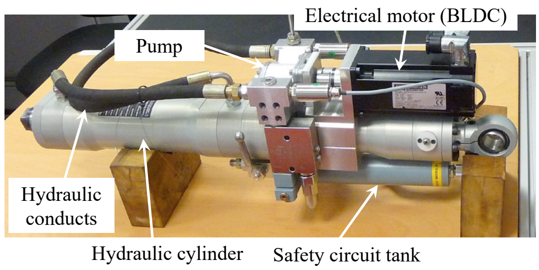

Fig. 2. Experimental setup components.

hydraulic actuator does not need any oil flow from any external power supply with the elimination of the oil pipe normally used to deliver power to the cylinder.

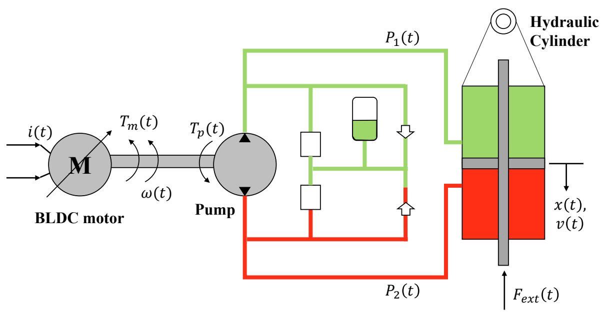

Fig. 3. Schematic of the EHSA system, with highlighted variables: quadrature current $i(t)$, motor torque $T_m(t)$, motor speed ω, pump torque $T_p(t)$, pressures $P_1(t), P_2(t)$, external force $F_{ext}(t)$ and rod position and speed $x(t), v(t)$.

An accurate linear and nonlinear model of the system has been presented in Belloli et al. (2010). The linearized model can be expressed as:

$$\begin{cases} \dot{\omega}(t) = \dfrac{1}{J_m}\big(-B_{fm}\cdot\omega(t) - D\cdot\Delta P(t) + K_t\cdot i_m(t)\big) \\ \Delta\dot{P}(t) = 2\dfrac{\beta_f}{V}\big(-K_L\cdot\Delta P(t) + D\cdot\omega(t) - A\cdot v(t)\big) \\ \dot{v}(t) = \dfrac{1}{M}\big(A\cdot\Delta P(t) - B_{fr}\cdot v(t) - F_{ext}(t)\big), \end{cases} \tag{25}$$

where J_m is the BLDC motor inertia, B_{fm} is the motor viscous friction, D is the pump displacement, K_t is the motor torque constant, K_L is the pump leakage coefficient, V is the average volume of oil in a cylinder chamber, A is the useful area of the hydraulic cylinder and B_{fr} is cylinder rod viscous friction. The system (25) presents:

- *2 inputs*: the BLDC motor quadrature current $i_m(t)$ which will act as a control variable; the external load force $F_{ext}(t)$, which is an external disturbance;
- *3 state variables*: the motor rotation speed $\omega(t)$, the differential pressure $\Delta P(t) = P_1(t) - P_2(t)$ in the cylinder chambers; the speed $v(t)$ the cylinder rod;
- *2 measured outputs*: the motor rotational speed $\omega(t)$ and the cylinder rod linear speed $v(t)$, obtained measuring the rod linear position.

The aim is to estimate the function $G_0(s) = \Omega(s)/I(s)$, where $\Omega(s) = \mathcal{L}[\omega](s)$ and $I(s) = \mathcal{L}[i](s)$, i.e. between the current reference and the BLDC motor speed, i.e.

$$N(s) = \frac{K_t}{J_m}\cdot\left[\left(s + \frac{2\beta_f}{V}K_L\right)\cdot\left(s + \frac{B_{fr}}{m}\right) + \frac{2\beta_f}{V}A^2\frac{1}{m}\right]$$

$$D(s) = \left(s + \frac{B_{fr}}{J}\right)\cdot\left(s + \frac{2\beta_f}{V}K_L\right)\cdot\left(s + \frac{B_{fm}}{m}\right) + \frac{2\beta_f}{V}A^2\frac{1}{m}\cdot\left(s + \frac{B_{fr}}{J_m}\right) + \frac{2\beta_f}{V}D^2\frac{1}{J}\cdot\left(s + \frac{B_{fm}}{m}\right)$$

$$G_0(s) = N(s)/D(s), \tag{26}$$

so that $G_0(s)$ has two zeros and three poles.

We performed open-loop experiments using a step current input of 1.25 A amplitude and measuring the motor rotational speed output, with a sampling frequency of $f_s = 200$ Hz, see Figure 4.

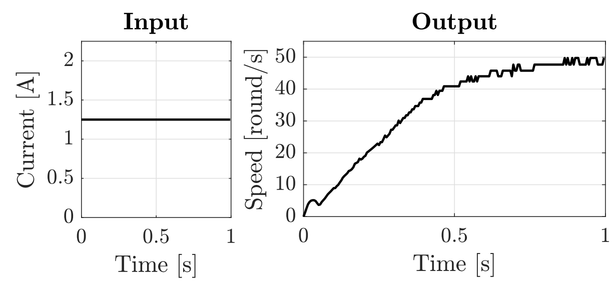

Fig. 4. Step input and output data used for identification.

The proposed *black-box* approach is compared with a *gray-box* approach that makes use of the knowledge of the system structure (25). The gray-box estimate is obtained by minimizing the squared error between measured and simulated output data. The simulated (gray-box) output data are obtained by feeding the (measured) step input to the parametric model (26). The simulation error is minimized using the `fmincon` MatLab command with the constraint that all parameters $J_m, B_{fr}, V, K_L, m, B_{fm}, Kt$, D, A, β_f, τ_d have to be positive.

The step response results are reported in Figure 5, where we simulated the identified models (gray-box and black-box) using two different step inputs of the same amplitude. Notice how, due to the system nonlinearities (mainly friction) and noise, the measured data are not the same. However, the proposed method, even if does not assume to know the system structure, performs better than the gray-box approach thanks to its flexibility. The black-box model corresponds to a transfer function of a 16th order. We reduced it using `balred` to the 3rd order to make it comparable with the gray-box model. Even in this case, the proposed method appears superior.

Figure 6 depicts the Bode diagrams of the estimated transfer functions. Both attain a very similar DC gain of about 40, while the dominant pole is around 1 Hz for all systems. The 16th order model obtained with the proposed method is clearly able to describe more accurately the system dynamics, where its pole attains a natural frequency up to 10 Hz. The reduced 3rd order model is a compromise between the gray-box one and the 16th order model. The model estimates are compared by the FIT index

$$\text{FIT} = \left(1 - \frac{\|\hat{y(t)} - y(t)\|_2}{\|y(t) - \bar{y}\|_2}\right)\cdot 100, \tag{27}$$

where $\hat{y}(t), y(t), \bar{y}$ are respectively the estimated, measured and average measured output, respectively.

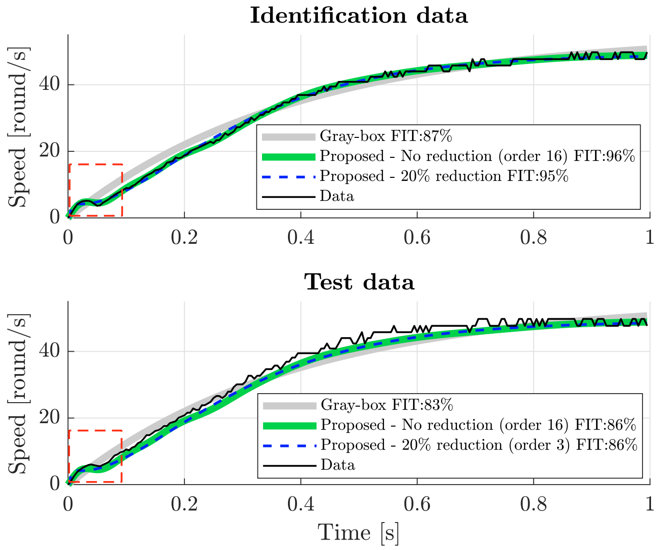

Fig. 5. Step responses on identification and test data. The highlighted initial transient dynamics is not captured by the gray-box model.

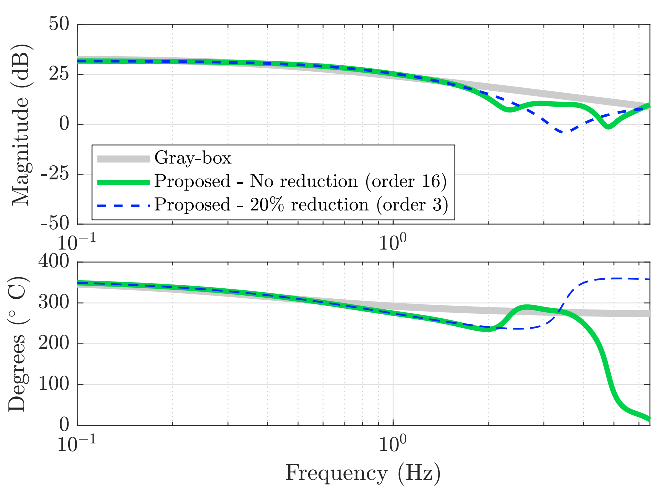

Fig. 6. Bode plots of the estimates transfer functions.

5. CONCLUSIONS

In this paper, we presented the computational aspects of a proposed algorithm black-box nonparametric algorithm for the estimation of continuous-time transfer function of SISO LTI models. The methodology was tested on an experimental setup and compared with a simulation error minimization gray-box identification scheme. The proposed approach showed superior performance even when using a low-exciting (but very commonly employed) input such as the step. Future research will be devoted to the analysis of different case studies and the extension of the analysis to other more general excitation signals.

REFERENCES

Baker, G.A. and Graves-Morris, P. (1996). *Padé approximants*, volume 59. Cambridge University Press.

Belloli, D., Previdi, F., Savaresi, S.M., Cologni, A., and Zappella, M. (2010). Modeling and identification of an electro-hydrostatic actuator. *IFAC Proceedings Volumes*, 43(18), 620–625.

Chen, F., Garnier, H., and Gilson, M. (2015). Robust identification of continuous-time models with arbitrary time-delay from irregularly sampled data. *Journal of Process Control*, 25, 19–27. doi:10.1016/j.jprocont.2014.10.003.

Dinuzzo, F. (2015). Kernels for linear time invariant system identification. *SIAM Journal on Control and Optimization*, 53(5), 3299–3317. doi:10.1137/130920319.

Dinuzzo, F. and Schölkopf, B. (2012). The representer theorem for hilbert spaces: a necessary and sufficient condition. In F. Pereira, C.J.C. Burges, L. Bottou, and K.Q. Weinberger (eds.), *Advances in Neural Information Processing Systems 25*, 189–196. Curran Associates, Inc.

Formentin, S., Mazzoleni, M., Scandella, M., and Previdi, F. (2019). Nonlinear system identification via data augmentation. *Systems & Control Letters*, 128, 56 – 63. doi:10.1016/j.sysconle.2019.04.004.

Garnier, H. and Gilson, M. (2018). CONTSID: a matlab toolbox for standard and advanced identification of black-box continuous-time models. *IFAC-PapersOnLine*, 51(15), 688–693. doi:10.1016/j.ifacol.2018.09.203. 18th IFAC Symposium on System Identification SYSID 2018.

Garnier, H. (2015). Direct continuous-time approaches to system identification. overview and benefits for practical applications. *European Journal of Control*, 24, 50 – 62. doi:10.1016/j.ejcon.2015.04.003. SI: ECC15.

Garnier, H. and Wang, L. (2008). *Identification of Continuous-time Models from Sampled Data*. Springer London. doi:10.1007/978-1-84800-161-9.

Golub, G.H. (2013). *Matrix Computations*. J. Hopkins Uni. Press.

Lofberg, J. (2004). Yalmip: a toolbox for modeling and optimization in matlab. In *2004 IEEE International Conference on Robotics and Automation (IEEE Cat. No.04CH37508)*, 284–289. doi:10.1109/CACSD.2004.1393890.

Mazzoleni, M., Scandella, M., Formentin, S., and Previdi, F. (2020). Black-box continuous-time transfer function estimation with stability guarantees: a kernel-based approach. *2nd Learning for Dynamics and Control Conference L4DC*.

Pillonetto, G. and De Nicolao, G. (2010). A new kernel-based approach for linear system identification. *Automatica*, 46(1), 81–93. doi:10.1016/j.automatica.2009.10.031.

Scandella, M., Mazzoleni, M., Formentin, S., and Previdi, F. (2020a). Kernel-based identification of asymptotically stable continuous-time linear dynamical systems. *International Journal of Control*, 1–29.

Scandella, M., Mazzoleni, M., Formentin, S., and Previdi, F. (2020b). A note on the numerical solutions of kernel-based learning problems. *IEEE Transactions on Automatic Control*, 1–1. doi:10.1109/TAC.2020.2989769.

Scandella, M., Mazzoleni, M., Formentin, S., and Previdi, F. (2020c). A note on the numerical solutions of kernel-based learning problems. *IEEE Transactions on Automatic Control*.

Varga, A. (1991). Balancing free square-root algorithm for computing singular perturbation approximations. In *Proceedings of the 30th IEEE Conference on Decision and Control*, volume 2, 1062–1065. IEEE. doi:10.1109/CDC.1991.261486.

Young, P.C. (2011). *Recursive Estimation and Time-Series Analysis*. Springer Berlin Heidelberg. doi:10.1007/978-3-642-21981-8.